

Effects of Inlet Distorted Flows on the Performance of an Axial Compressor

Asad Islam, Khalid Parvez

Abstract—Compressor fans in modern aircraft engines are of considerable importance, as they provide majority of thrust required by the aircraft. Their challenging environment is frequently subjected to non-uniform inflow conditions. These conditions could be either due to the flight operating requirements such as take-off and landing, wake interference from aircraft fuselage or cross-flow wind conditions. So, in highly maneuverable flights regimes of fighter aircrafts affects the overall performance of an engine. Since the flow in compressor of an aircraft application is highly sensitive because of adverse pressure gradient due to different flow orientations of the aircraft. Therefore, it is prone to unstable operations.

This paper presents the study that focuses on axial compressor response to inlet flow orientations for the range of angles as 0 to 15 degrees. For this purpose, NASA Rotor-37 was taken and CFD mesh was developed. The compressor characteristics map was generated for the design conditions of pressure ratio of 2.106 with the rotor operating at rotational velocity of 17188.7 rpm using CFD simulating environment of ANSYS-CFX®. The grid study was done to see the effects of mesh upon computational solution. Then, the mesh giving the best results, (when validated with the available experimental NASA's results); was used for further distortion analysis. The flow in the inlet nozzle was given angle orientations ranging from 0 to 15 degrees. The CFD results are analyzed and discussed with respect to stall margin and flow separations due to induced distortions.

Keywords—Angle, ANSYS-CFX®, axial compressor, Bladegen®, CFD, distortions.

I. INTRODUCTION

AXIAL flow compressors in aircrafts, gas turbine engines or other applications are often subjected to intense flow distortions at the inlet, which affects the overall performance of the compressor. Distortions sometimes become so sensitive for compressor's operation that it might fail causing the overall installation mechanism to blow off.

Carta [1] suggested two hypothetical inlet distortions as function of relative rotor incidence angle with the circumferential location. The first type of distortions is called as the forward traverse; which has a rapidly increasing and then slowly decreasing incidence flow angle. The second type of distortion is called as backward traverse, which is opposite to the former one. Katz [2] also experimentally performed the distortions analysis for a 3-stage axial compressor and his results showed that inception of the rotating stall was almost unaffected by the inlet disturbance. This was because of the

fact that the inlet distortions attenuated very rapidly through the compressor to the last stage, which was possibly responsible for the onset of rotating stall, and it operated in almost uniform flow.

There are different ways by which researchers had introduced inlet perturbations in axial compressors experimentally. A simple and easy way to create perturbations is to install a distortion screen made up of wire gauze or similar material at the upstream of the compressor [2]-[4]. Uniform screens generate a square wave distortion and experimental studies with this procedure had already been studied. As an example, [5] has investigated a 60 degrees-square wave inlet flow distortion using the same methodology. A. Mushtaq [6], [7] also performed research on the stability of the transonic axial flow compressor by tip injections of different mass flows. His results showed that maximum injection of mass flow aligned with the blade camber helps in maximizing the stability while minimizing the performance penalties. However, this paper describes the CFD simulation of inlet distortions in an axial-compressor rotor by varying nozzle-inlet flow orientations by a range of 0 to 15 degrees, using the computational environment of ANSYS-CFX ® software package.

II. COMPRESSOR SPECIFICATIONS

The study focuses on the performance response to induced distortions by inlet flow orientations in an axial compressor rotor. For this purpose, NASA Rotor 37, an open test case; was taken for our concerned study. It is a transonic compressor rotor having 36 blades with a tip clearance of 0.356 mm and it revolves about the negative Z axis. The simulations were carried out for 100% N (i.e., 17188.7 rpm) and then the rotational speed was decreased to 80%N.

TABLE I
SPECIFICATIONS AND DESIGN CONDITIONS FOR AXIAL COMPRESSOR

Parameter	Size
Rotor inlet hub-to-tip diameter ratio	0.7
Rotor blade inlet tip radius	254 mm
Rotor Blade span	76.2 mm
Tip Clearance	0.356 mm
Tip Solidity	1.288
Design Conditions	
No. of Blades	36
Mass flow rate	20.93 kg/sec
Total pressure ratio	2.106
Rotational speed	17188 rpm

Asad Islam is affiliated with Department of Aeronautics and Astronautics, Institute of Space Technology, Islamabad, 44000, Pakistan (+92-51-9075659; email: engr.asad.islam@live.com)

Dr Khalid Parvez was with RCMS, NUST, Pakistan. He is now with the Department of Aeronautics and Astronautics, IST, Islamabad-44000, Pakistan (e-mail: khalid.parvez@ist.edu.pk).

All the CFD results were validated with the available experimental results before proceeding towards the distortion study. This CFD model validation was a benchmark for introducing inlet flow distortions and studying its effects on stall margin and corresponding flow separations.

The specifications of the above considered rotor are shown in Table I.

III. ROTOR CAD GEOMETRY

The geometry of axial compressor rotor was created according to the specifications listed in Table I using ANSYS-Bladegen® software; which is a specialized tool for turbomachinery blade designing. Single blade schematic is displayed in Fig. 1. Fig. 2 shows the CAD model of full rotor.

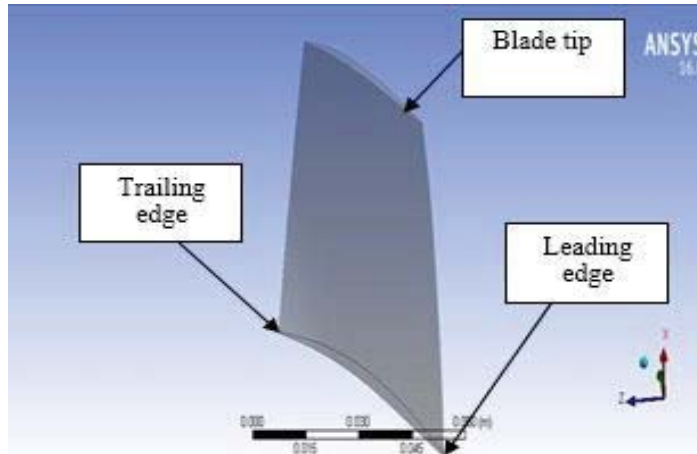


Fig. 1 Single Blade schematic view

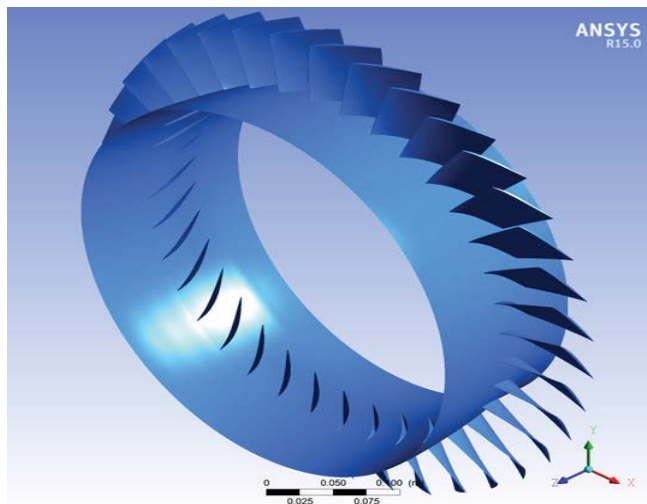


Fig. 2 Full rotor view

IV. GRIDS GENERATION

The grid was created using CFX-Turbogrid®, which provides an efficient tool for generating high quality hexahedral mesh.

The fine mesh is of considerable importance for a CFD analysis. Since there is internal flow of compressor, so, fine and appropriate grid size gives a good compromise between the accuracy and the computational time. The grid view of full rotor is displayed in Fig. 3.

In order to save the computational resources and time required to simulate the full rotor wheel, single rotor blade

passage was considered. A view of an isolated blade passage with its hub and shroud are shown in Fig. 4.

Table II shows the mesh information of both the mesh#01 and refined meshes.

TABLE II
MESHER INFORMATION OF AXIAL COMPRESSOR ROTOR

	No. of Nodes	No. of Elements
Mesh# 01	203220	191028
Refined Mesh	372620	353670

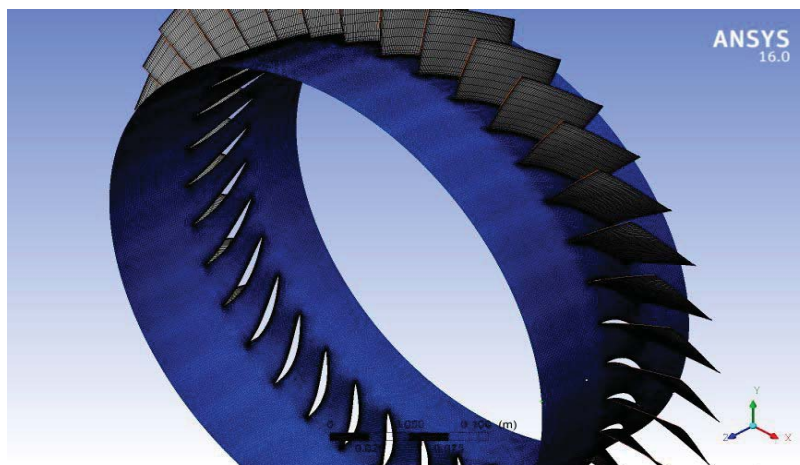


Fig. 3 Full rotor grid view

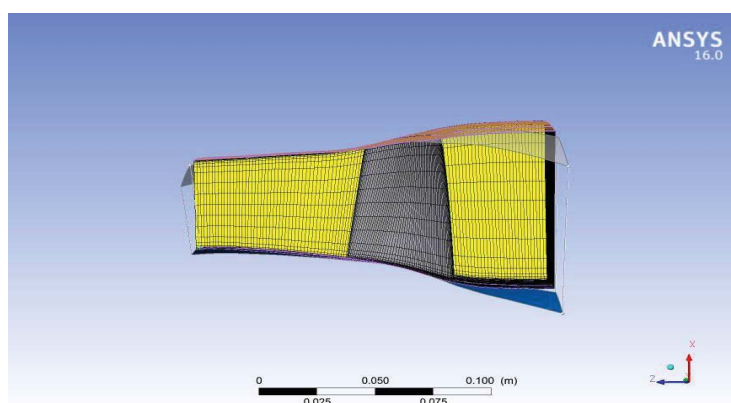


Fig. 4 Single passage (Hub, Blade & Shroud)

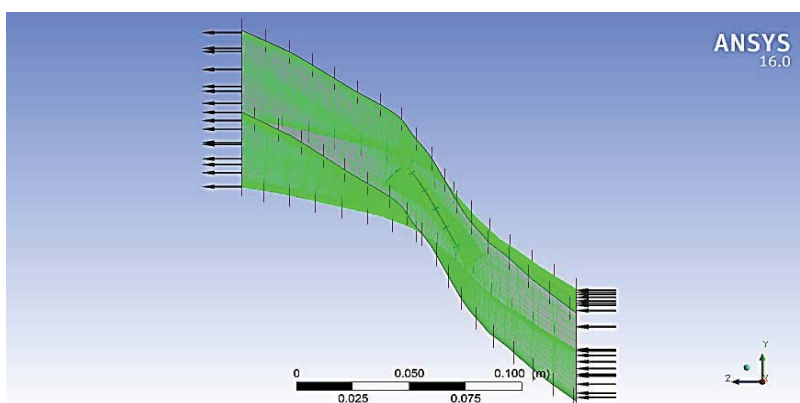


Fig. 5 Flow direction in blade passage (Inlet & Outlet)

V.CFD METHODOLOGY

The ANSYS CFX® solver was used as a simulating platform for obtaining CFD solution.

In the simulations, the design blade speed was 17188.7 rpm which is denoted as 100%N and then the speed was decreased from 100% N to 80% N to build the compressor map. However, in this paper, the distortion effects at 100% speed

were studied only. The distortions were created by implementing flow orientations at the inlet as 5°, 10° and 15°. The compressor rotor operating at design speed is near to stall at 10 degrees flow orientation and is stalled at the 15 degrees flow orientation; while maintain the same mass flow and increasing the flow orientation.

VI. BOUNDARY CONDITIONS

The total pressure at the inlet is 1 atm and temperature of 288 K; while a back-pressure is implied at the outlet of the rotor, so that a compressor map can be built. All walls are modeled as adiabatic and with no slip conditions.

The blade passage flow directions at the inlet and outlet is shown in Fig. 5.

VII. GRID STUDY AND VALIDATION OF CFD MODEL

For the purpose to visualize the effects on the solution by refining the grids, two different meshes were developed and the resulting solution was compared with the experimental results. Fig. 6 shows the mesh refinement study and validation of our CFD model.

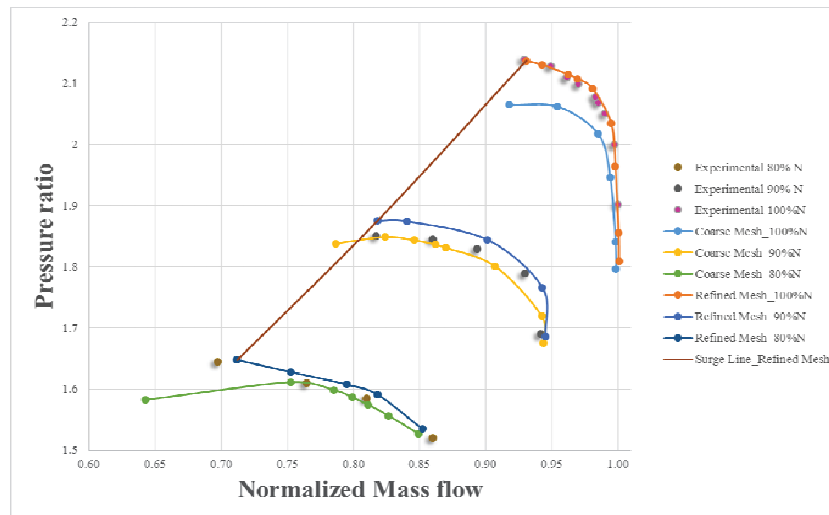


Fig. 6 Mesh study and CFD model validation

In Fig. 6, the refined results are highlighted with the surge line whereas, the experimental results are shown by dots.

at the blade leading and trailing edges upon flow orientations are shown.

VIII. RESULTS

In this section, the distortion effects on the pressure ratio and the polytropic efficiency and blade loading are expressed in terms of graphs shown as Figs. 5, 6, and 7 respectively. Whereas, the contours of pressure and relative Mach number

A. Compressor Characteristic Map

By giving the orientations to the flow at the inlet, the pressure ratio variations in the characteristic map are displayed in Fig. 7.

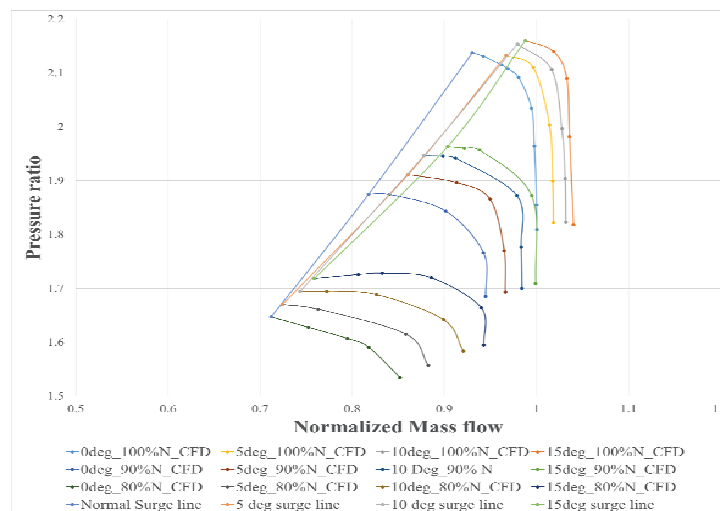


Fig. 7 Pressure ratio vs mass flow of distorted flows

B. Polytropic Efficiency at Distortions

The polytropic efficiency at design speed of 17188.7 rpm is shown in Fig. 8:

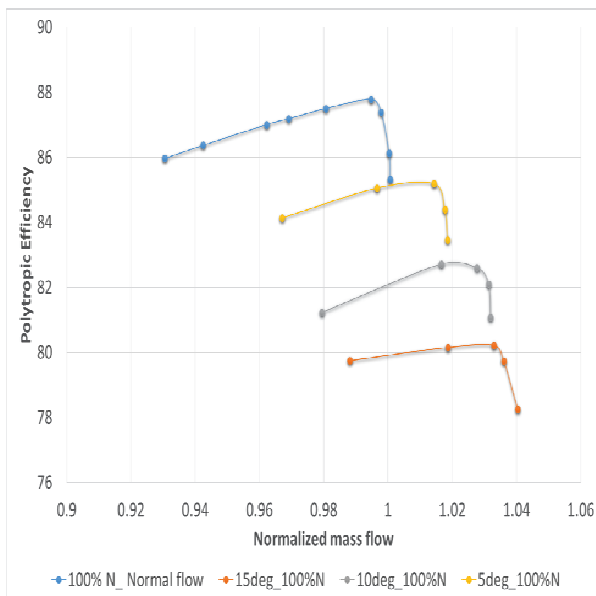


Fig. 8 Polytropic efficiency of distorted flows at 100%N

C. Blade Loading at 50% Span

Fig. 9 shows the blade loading at clean and normal operation at rotational speed of 17188.7 rpm.

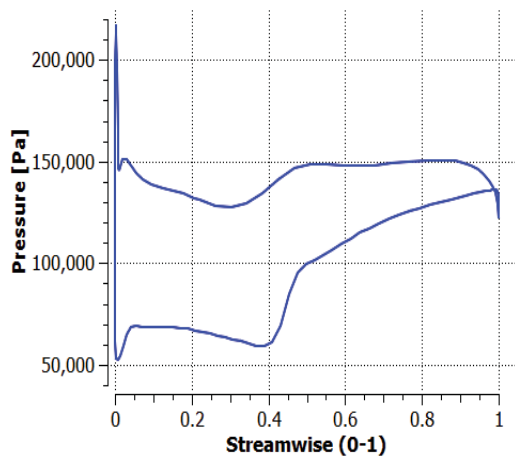


Fig. 9 Blade loading at clean flow

Fig. 10 shows the blade loading at 5 degrees inlet flow orientation at rotational speed of 17188.7 rpm under normal operation.

Fig. 11 shows the blade loading at **near stall** 10 degrees inlet flow orientation at rotational speed of 17188.7 rpm

Fig. 12 shows the blade loading at stall and 15 degrees inlet flow orientation at rotational speed of 17188.7 rpm

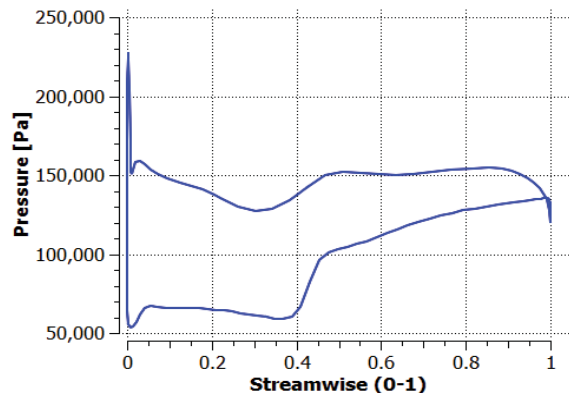


Fig. 10 Blade loading at 5 degree flow orientation

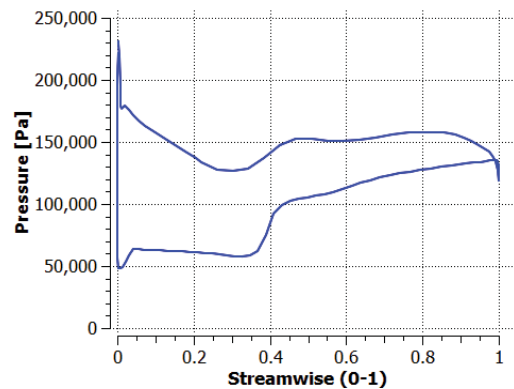


Fig. 11 Blade loading at near stall (10 degrees flow orientation, NEAR STALL)

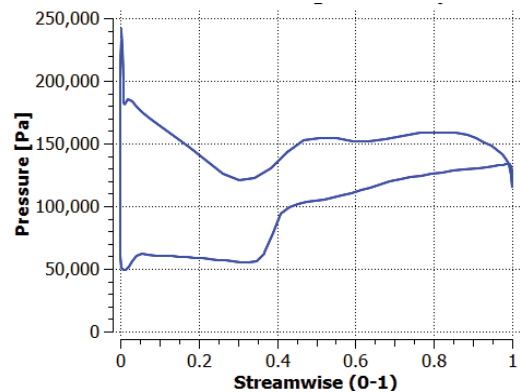


Fig. 12 Blade loading at Stall condition (15 degrees flow orientation, STALLED)

D. Pressure at Blade LE

Figs. 13-16 show the pressure contours at the Blade leading edge. The compressor rotor operating at design speed is near to stall at 10 degrees flow orientation and is stalled at the 15 degrees flow orientation; while maintain the same mass flow and increasing the flow orientation.

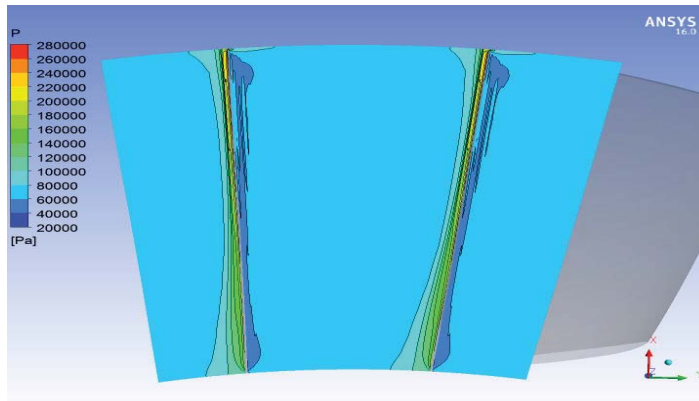


Fig. 13 Pressure contours at Blade LE (Normal flow without distortion)

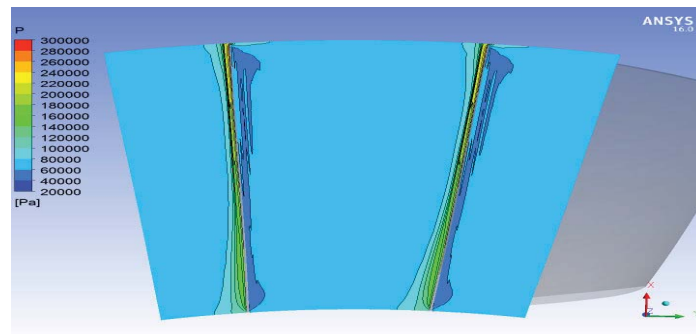


Fig. 14 Pressure contours at Blade LE (5 degrees flow orientation)

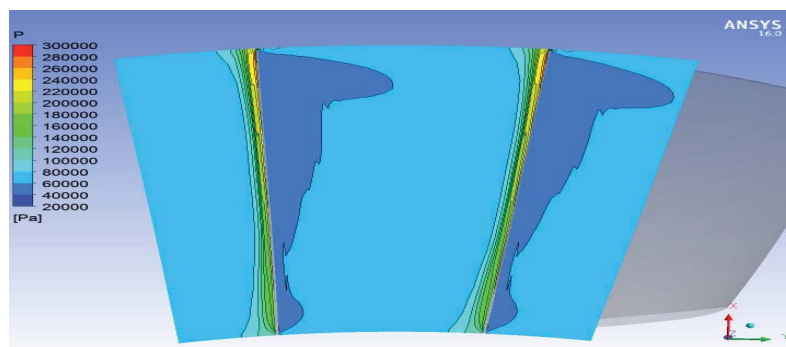


Fig. 15 Pressure contours at Blade LE (10 degrees flow orientation, Near Stall)

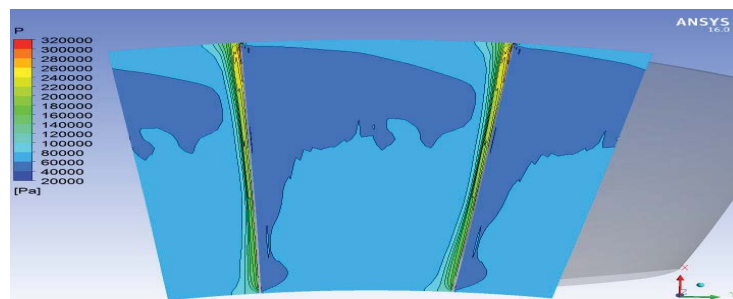


Fig. 16 Pressure contours at Blade LE (15 degrees flow orientation, Stall)

E. Pressure at Blade TE

Figs. 17-20 show the pressure contours at the Blade trailing edge. The compressor rotor operating at design speed is near

to stall at 10 degrees flow orientation and is stalled at the 15 degrees flow orientation; while maintain the same mass flow and increasing the flow orientation.

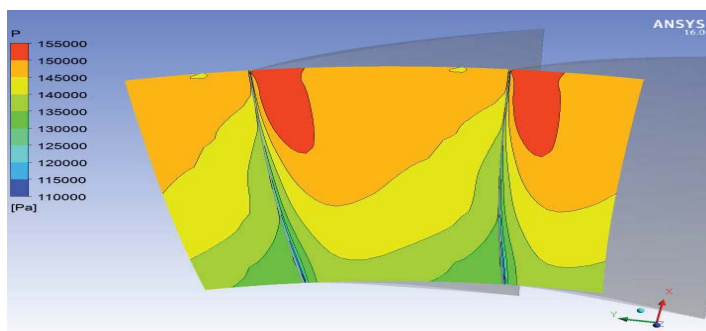


Fig. 17 Pressure contours at Blade TE (Normal flow)

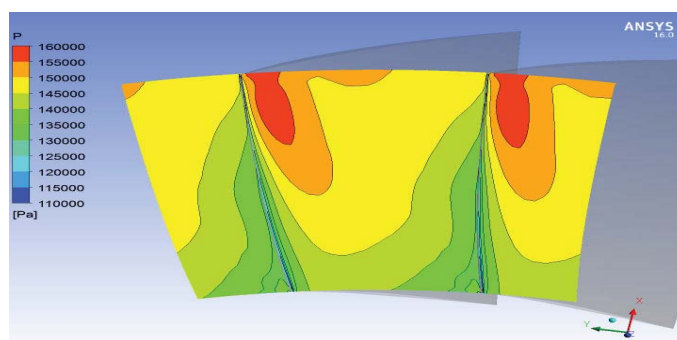


Fig. 18 Pressure contours at Blade TE (5 degrees flow orientation)

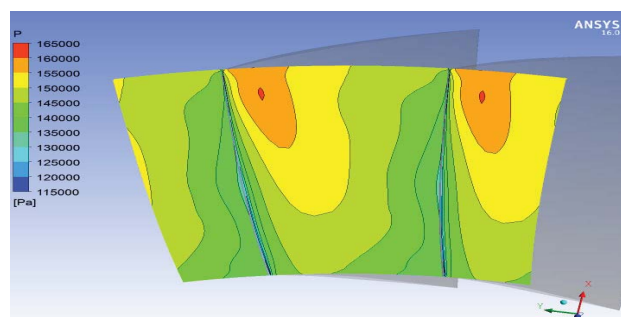


Fig. 19 Pressure contours at Blade TE (10 degrees flow orientation, Near Stall)

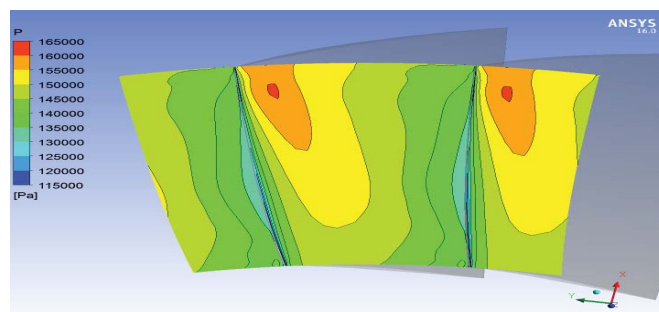


Fig. 20 Pressure contours at Blade TE (15 degrees flow orientation, Stall)

F. Relative Mach at Blade LE

Figs. 21-24 show the relative Mach number contours at the Blade leading edge. The compressor rotor operating at design

speed is near to stall at 10 degrees flow orientation and is stalled at the 15 degrees flow orientation; while maintain the same mass flow and increasing the flow orientation.

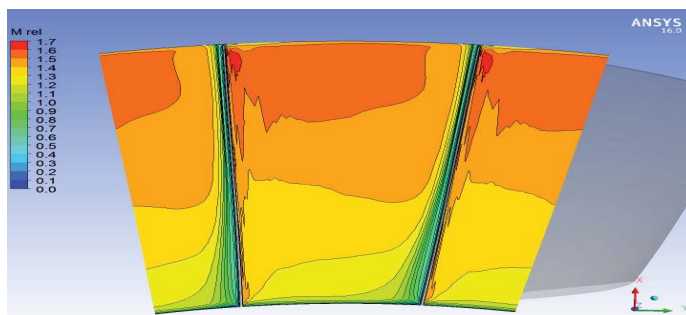


Fig. 21 Relative Mach No. contours at Blade LE (Normal flow)

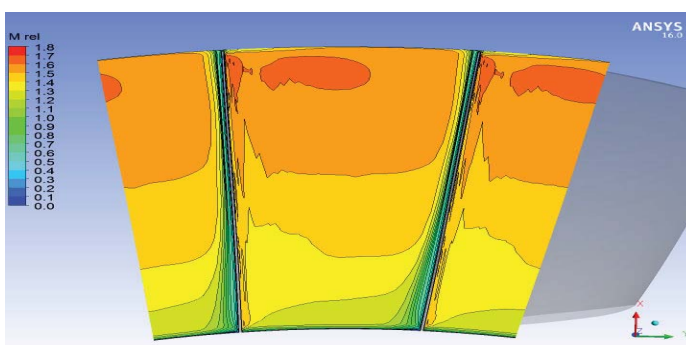


Fig. 22 Relative Mach No. contours at Blade LE (5 degrees flow orientation)

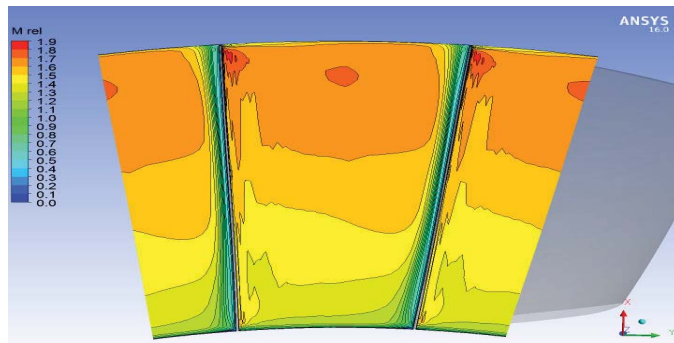


Fig. 23 Relative Mach No. contours at Blade LE (10 degrees flow orientation, Near Stall)

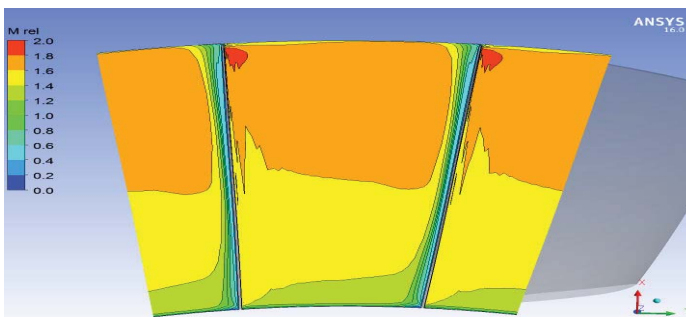


Fig. 24 Relative Mach No. contours at Blade LE (15 degrees flow orientation, Stall)

G. Relative Mach at Blade TE

Figs. 25-28 show the relative Mach number contours at the Blade leading edge. The compressor rotor operating at design

speed is near to stall at 10 degrees flow orientation and is stalled at the 15 degrees flow orientation; while maintain the same mass flow and increasing the flow orientation.

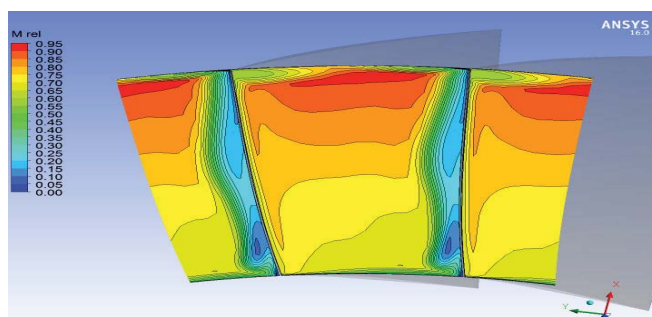


Fig. 25 Relative Mach No. contours at Blade TE (Normal flow)

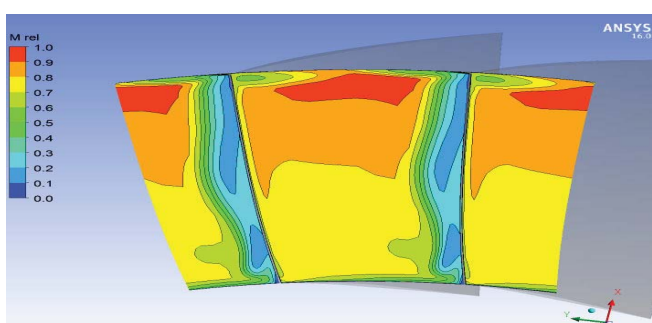


Fig. 26 Relative Mach No. contours at Blade TE (5 degrees flow orientation)

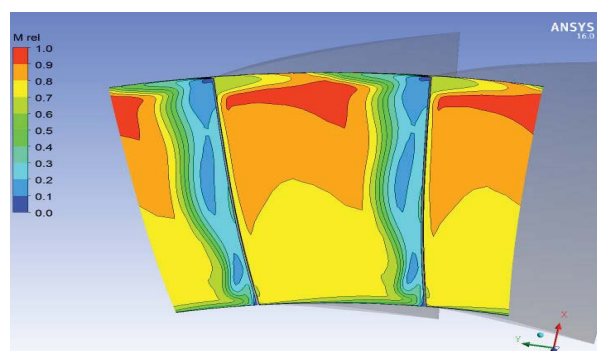


Fig. 27 Relative Mach No. contours at Blade TE (10 degrees flow orientation, Near Stall)

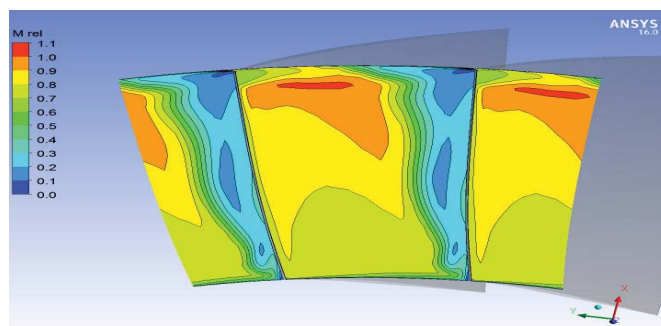


Fig. 28 Relative Mach No. contours at Blade TE (15 degrees flow orientation, Stall)

IX.CONCLUDING REMARKS

Different flow orientations were utilized as a strategy to introduce distortions in an axial compressor. By increasing the flow orientations from 0 degrees to 15 degrees while keeping the same mass flow, it was seen that

1. At 10 degrees, the rotor is near to stall while at 15 degrees, the compressor stalls. Whereas, at 0 and 5 degrees, the compressor performs normal although small distortion is there.
2. The surge line shifts making the stall margin to decrease as depicted in Fig. 7.
3. The polytropic efficiency decreases, which is a clear sign of distorted performance, as depicted from Fig. 8.
4. Blade loading at 50% span is increasing near 0.6-0.8 streamwise on the pressure surface of the blade while decreasing on the suction surface near 0.2-0.4 streamwise as the flow is distorting.
5. Furthermore, the high flow separations were also observed due to which the stall margin decreases as the flow at the inlet creating disturbances.

REFERENCES

- [1] F. O. Carta, "Unsteady normal force on an airfoil in a periodically stalled inlet flow", *Journal of Aircraft*, Vol.4, No.5, p.416, 1967.
- [2] R. Kartz, Performance of axial compressors with asymmetric inlet flows, Guggenheim Jet Propulsion Centre, Cal. Inst. Tech. Report. 1958.
- [3] F. Roberts, G. A. Plourde and F. Smakula, "Insights into axial compressor response to distortion", AIAA Paper No.68-565, 1969.
- [4] R. C. Turner, J. Ritchie and C. E. Moss, "The effect of inlet circumferential maldistribution on an axial compressor stage", ARC R. & M. No.3066, 1957.
- [5] H. Mook, "The Unsteady Response of an Axial Flow Compressor with a distorted Inlet Flow", C.P No. 1203, Ministry of Defence (Procurement Executive), Aeronautical Research Council.
- [6] U. Farooq, J. Masud, S. Ahmed, K. Parvez, J. A. Khan, A. Mushtaq "Assessment of Commercial CFD Codes for Performance Prediction of Transonic Axial Compressor", Proceedings of AMSE Turbo Expo 2011, GT2011-45006, Vancouver Canada.
- [7] A. Mushtaq, K. Parvez, S. Ahmed and J. A. Khan, "Parametric study of tip injection on the stability of transonic axial flow compressor", 49th American Institute of Aeronautics and Astronautics.